Eur J Nucl Med Mol Imaging (2007) 34:S86–S98
DOI 10.1007/s00259-007-0443-0

Cardiovascular molecular imaging of apoptosis

S. L. Wolters · M. F. Corsten · C. P. M. Reutelingsperger · J. Narula · L. Hofstra

Published online: 6 June 2007

Abstract
Introduction Molecular imaging strives to visualise processes at the molecular and cellular level in vivo. Understanding these processes supports diagnosis and evaluation of therapeutic efficacy on an individual basis and thereby makes personalised medicine possible.
Apoptosis and molecular imaging Apoptosis is a well-organised mode of cell suicide that plays a role in cardiovascular diseases (CVD). Apoptosis is associated with loss of cardiomyocytes following myocardial infarction, atherosclerotic plaque instability, congestive heart failure and allograft rejection of the transplanted heart. Thus, apoptosis constitutes an attractive target for molecular imaging of CVD. Our current knowledge about the molecular players and mechanisms underlying apoptosis offers a rich palette of potential molecular targets for molecular imaging. However, only a few have been successfully developed so far.
Aims This review highlights aspects of the molecular machinery and biochemistry of apoptosis relevant to the development of molecular imaging probes. It surveys the role of apoptosis in four major areas of CVD and portrays the importance and future perspectives of apoptosis imaging. The annexin A5 imaging protocol is emphasised since it is the most advanced protocol to measure apoptosis in both preclinical and clinical studies.

Keywords Apoptosis · Molecular imaging · Cardiovascular disease · Annexin A5

S. L. Wolters · C. P. M. Reutelingsperger
Department of Biochemistry, Cardiovascular Research Institute Maastricht, Maastricht University,
Maastricht, The Netherlands

J. Narula
Department of Cardiology, University of California Irvine,
Irvine, USA

M. F. Corsten · L. Hofstra (✉)
Department of Cardiology, Cardiovascular Research Institute Maastricht, Maastricht University,
P.O. Box 616, Maastricht 6200 MD, The Netherlands
e-mail: l.hofstra@cardio.unimaas.nl

Apoptosis

The term ‘apoptosis’ is derived from the Greek (*apo* = from and *ptosis* = falling, commonly pronounced ap-a-tow’-sis) and denotes a regulated process of cell suicide resulting in a cell corpse that is distinct from the necrotic cell [1, 2]. Whereas necrosis is manifested by cellular swelling, plasma membrane rupture and rapid release of intracellular constituents into the environment, causing an inflammatory response [2], apoptosis is characterised by cell shrinkage, long-lasting maintenance of plasma membrane integrity and lack of inflammatory responses in the vicinity of the dying cell [2]. It has long been thought that apoptosis and necrosis are the only two modes of cell death counterbalancing mitosis [3]. However, recent insights have taught us that cells can follow more roads to death than only apoptosis and necrosis. In 2001, Leist and Jaättelä suggested a model in which various forms of cell death could be positioned on a gliding scale between two extremes, apoptosis and necrosis [4]. The mode of execution depends on the cell type and the cell death-inducing trigger. Most knowledge about various modes of cell death has been generated in the field of oncology, where cell death plays an important role in the progression and treatment of cancer [5]. Several intermediate forms of cell death have been identified and

characterised [6, 7], including mitotic catastrophe and autophagic cell death. Mitotic catastrophe can be the result of unsuccessful chromosome segregation, an event that requires malfunctioning of multiple cell cycle checkpoints. Catastrophic cells are large and non-viable cells with a compromised nuclear blueprint leading eventually to cell death [8]. Mitotic catastrophe appears to be a rare event in cardiovascular diseases. Autophagic cell death is characterised by the total destruction of the cell through autophagy. It is a process in which cytoplasmic constituents are degraded through the lysosomal machinery [9]. Autophagic cell death occurs both in oncology [10, 11] and in cardiovascular diseases [12]. The various described modes of cell death differ in morphology and biochemistry [13]. The caspase cascade is the most remarkable biochemical distinction [14]. It is activated during apoptosis but hardly, or not at all, during other modes of cell death.

Biochemistry of apoptotic cell death

Two major biochemical routes dominate apoptotic cell death. They involve the activation of the caspase cascade through either death-receptor mediated signal transduction or stress-induced release of cytochrome C from mitochondria [15]. Caspases involved in apoptosis can be grouped into initiator (caspases 8 and 9) and effector caspases (caspases 3 and 7). The principal event of the caspase cascade is the activation of an inactive procaspase into a proteolytically active caspase. Activation of initiator caspases occurs through auto-activation, catalysed by the interaction with ligated death receptors (procaspase 8) or cytochrome C-containing apoptosome (procaspase 9). Effector caspases are activated through intra-chain cleavage by active initiator caspases [16]. In both cases, activation results in the exposure of active sites that selectively cleave peptide bonds after an aspartate residue in caspase substrates.

Several checks and balances exist that control burst of the caspase cascade if triggered by minor undesired initiating events. Inhibitors of apoptotic proteins (IAPs) suppress proteolytic activity by binding to activated caspases. Inhibition of IAPs is in turn required to allow execution of apoptosis. Smac/DIABLO residing in the mitochondria and co-released with cytochrome C inhibits IAPs and permits propagation and amplification of the proteolytic signal through the caspase cascade. Anti-apoptotic members of the Bcl-2 family such as Bcl-2 and Bcl-X prevent the release of cytochrome C and Smac/DIABLO from mitochondria. Pro-apoptotic members such as Bax and tBid, which is the result of Bid cleavage by activated caspase 8, neutralise the protective effects of the anti-apoptotic members and provoke mitochondria to release their pro-apoptotic cargo.

The intricate scheme of the apoptotic machinery offers several potential targets for molecular imaging. For example, knowledge about the mechanism of caspase activation has triggered the design of several strategies to measure apoptosis [17–19]. The hurdle these methods have to take is entrance of the reporter of caspase activity into the cell. Consequently, in vivo applications of such strategies face unfavourable biodistribution profiles and high background levels. Targets embedded in the plasma membrane encompass a more promising set of molecules for molecular imaging.

Phosphatidylserine

An essential part of the apoptotic program consists of the appearance of ‘eat me’ flags at the cell surface. Phagocytes recognise these flags and respond by engulfing the dying cell before it leaks pro-inflammatory components into the surrounding tissue. The ‘eat me’ flags are, alone or in combination, specific for the dying cell, allowing phagocytes to make the right choice in an environment filled with living cells.

In 1992, Valerie Fadok and co-workers reported that phosphatidylserine (PS) becomes exposed on the surface of apoptotic lymphocytes, where it functions as an ‘eat me’ signal for phagocytes [20]. PS, a negatively charged aminophospholipid, is predominantly found in the cytofacial membrane leaflets of living cells. The exofacial plasma membrane leaflet contains predominantly phosphatidylcholine and sphingomyelin while PS is almost completely lacking. The PS asymmetry results from the ATP-dependent action of the aminophospholipid translocase that transports PS from the outer to the inner leaflet [21, 22]. During apoptosis the aminophospholipid translocase is inhibited and concomitantly a scramblase is activated. The combined action results in the surface expression of PS whilst the plasma membrane integrity remains intact.

Surface-expressed PS provides an attractive target for molecular imaging of apoptosis.

Annexin A5

In the past decade, a molecular imaging protocol was established to detect and measure apoptosis in vitro and in vivo in animal models and patients [23–26]. This molecular imaging protocol is based upon the protein annexin A5 (Anx A5), which binds with high selectivity and with great affinity (K_a=7 n*M*) [27, 28] to the PS abnormally expressed on the cell membrane of apoptotic cells [21, 22, 29]. Anx A5 is a member of a multiprotein family of more than 160 proteins that share the property of Ca^{2+}-dependent binding

to negatively charged phospholipid surfaces [30]. The biophysical, biochemical and biological properties of Anx A5 and other members of the annexin family have been extensively described in a number of excellent reviews [30–34].

Detecting apoptosis with Anx A5

The development of annexin-based detection of apoptosis started in 1992 when Fadok et al. revealed that PS is expressed on the cell surface of apoptotic cells [35]. This revelation led Koopman et al. to the design of an apoptosis detection assay on the basis of fluorescence (fluorescein isothiocyanate)-labelled Anx A5 [29]. This Anx A5 affinity assay was further developed by labelling Anx A5 with biotin or with several radionuclides to facilitate various protocols for measuring apoptosis both in vitro [36] and in vivo [23–25, 37–41] in animal models. The availability of ^{99m}Tc-labelled Anx A5 produced under GMP regulations led to the first studies of non-invasive detection of apoptosis in patients [26, 42–46].

Detection of apoptosis using alternative methods

In addition to Anx A5, several other proteins may have a high specificity and tight binding to PS. If labelled with a fluorescent or nuclear probe, these proteins could possibly be used for in vivo detection of apoptotic cells in the field of cardiovascular disease and in other disciplines. In addition, other steps in the apoptotic signalling cascade, such as the activation of caspase-3, can be utilised to visualise activation of the apoptotic machinery (Fig. 1).

Synaptotagmin I

One such PS binding protein is the C2 domain of synaptotagmin I, which binds to anionic phospholipids in cell membranes [47]. By conjugation of the C2 domain, synaptotagmin can be used for in vivo molecular imaging of apoptosis. Zhao and co-workers conjugated the C2 domain with superparamagnetic iron oxide (SPIO) particles, a very effective T2 relaxing MRI contrast agent, and injected the product in tumour-bearing mice. They revealed that a murine lymphoma (EL4) tumour model treated with cyclophosphamide and etoposide showed an increase in apoptotic cells from a basal value of 4% to 32% during chemotherapy. This was readily detected with C2-labelled SPIO particles and T2W MRI. Tumour regions with the greatest MRI changes correlated with regions having the highest proportion of apoptotic and necrotic cells [47]. More recently, the same group labelled the C2A domain of synaptotagmin I radioactively (^{99m}Tc) or fluorescently (FITC) and used the labelled synaptotagmin in a reperfused acute myocardial infarction model (AMI) rat model. They found both ex vivo and in vivo accumulation of the radiotracer in the area at risk. Although some of the uptake was caused by passive leakage due to elevated vascular permeability in the area at risk, the majority was caused by specific binding to PS [48].

Both Anx A5 and synaptotagmin I detect apoptotic cells by selective binding to externalised PS. An alternative method to detect apoptosis may be to use a target more upstream in the apoptotic cascade, the effector caspases.

5-Pyrrolidinylsulphonyl isatins

In one study the peptide-based irreversible pan-caspase inhibitor Z-VAD-fmk was radio-iodinated and suggested as

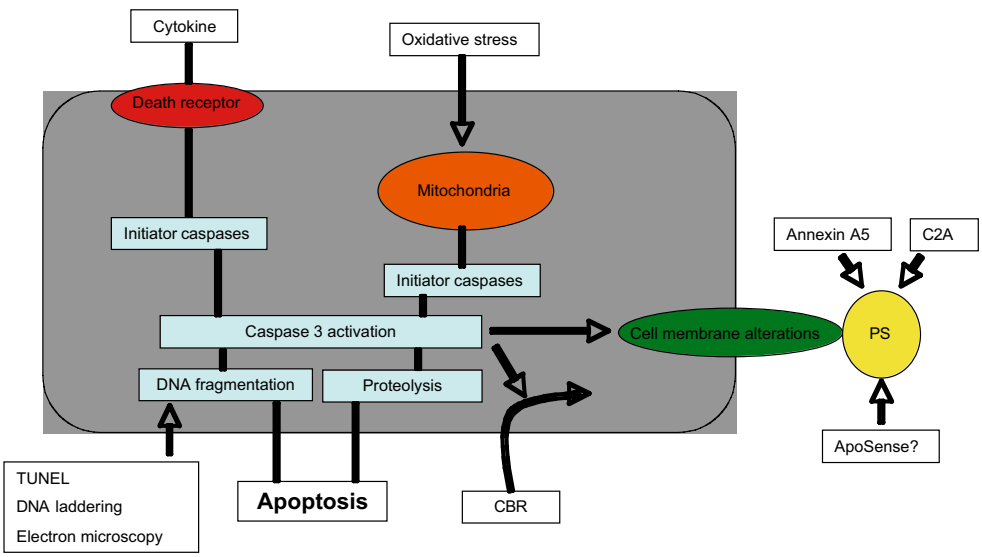

Fig. 1 Targets for apoptosis detection. During apoptosis, initiator caspases are activated, via either cell death receptor-mediated or mitochondrial signalling. These initiator caspases, in turn, trigger the activation of effector caspases, such as caspase-3. The activation of caspase-3 results in the typical characteristics of apoptosis, such as DNA fragmentation, substrate cleavage of cytoplasmic proteins and cell membrane alterations. These apoptotic characteristics and the activation of caspase-3 offer targets for molecular imaging of apoptosis

a caspase imaging agent. However, due to poor cellular permeability, intracellular targeting of activated caspases was limited, preventing in vivo application [49]. In more recent work, non-peptidyl caspase inhibitors of the 5-pyrrolidinylsulphonyl isatin-type were proposed instead of a peptide-based caspase, such as Z-VAD-fmk. These *c*aspase *b*inding *r*adioligands (CBRs) may be capable of directly targeting apoptosis in vivo. CBRs are expected to form intracellular enzyme inhibitor complexes by means of binding to the activated caspases. Kopka and co-workers succeeded in labelling several 5-pyrrolidinylsulphonyl isatins with iodine-125 [50]. However, none of these compounds have been used for non-invasive imaging in patients yet.

ApoSense

The ApoSense family is a group of low molecular weight amphipathic apoptosis markers targeting the cell membrane of apoptotic cells. ApoSense was developed by the Israel-based company NST. ApoSense has been used in vitro and in vivo in several disease models associated with cell death, such as radiation-induced lymphoma, renal ischaemia/reperfusion and cerebral stroke [51, 52]. However, it is still not known to which cell membrane target ApoSense exactly binds. Therefore, it remains a challenge to link ApoSense binding to the signalling cascades in apoptosis signalling.

Role and detection of apoptosis in CVD

Apoptosis of cardiomyocytes after myocardial infarction

Several forms of cell death have been observed in the infarcted myocardium. The central ischaemic zone is dominated by necrotic cell death, whereas in the periphery of the area at risk mainly apoptotic cell death is observed. Apoptotic cell death in the infarct periphery is not the exclusive domain of the cardiomyocyte. Also non-myocytes, including endothelial cells, macrophages and blood cells, contribute to a comparable degree to apoptotic cell death [53]. Since the process of cell death can be pharmaceutically manipulated, thereby limiting the extent of myocardial cell loss, detection and quantification of apoptotic cells are of importance for determination of the full extent of reversible myocardial damage. Once the apoptotic program is activated, several targets are present both for imaging apoptosis and for therapeutic interventions.

As described earlier, the C2A domain of synaptotagmin I binds to the exposed PS on apoptotic cells. Zhao and co-workers developed a radiotracer for PS expression by labelling synaptotagmin via 2-iminothiolane thiolation with ^{99m}Tc, forming a technetium C2A glutathione S-transferase complex (^{99m}Tc-C2A-GST) [48]. In vivo planar imaging of AMI in rats was performed on a gamma camera using a parallel-hole collimator. The uptake of ^{99m}Tc-C2A-GST within the area at risk was quantified by direct gamma counting. The foremost finding was that in seven of seven rats the infarct was clearly identifiable as focal uptake in planar images. This and other findings led the authors to conclude that the C2A domain of synaptotagmin I labelled with a radioisotope binds to both apoptotic and necrotic cells. Ex vivo and in vivo data indicate that, because of elevated vascular permeability, both specific binding and passive leakage contribute to the accumulation of the radiotracer in the area at risk. However, the latter component alone is insufficient to achieve detectable target-to-background ratios using in vivo planar imaging.

Annexin A5 has been more widely used to target PS exposure. Hiller and co-workers [54] recently reported on a new Anx A5-based T1 contrast agent. They linked Anx A5 to gadolinium diethylenetriamine penta-acetate (Gd-DTPA)-coated liposomes. In their model of perfused isolated rat heart, ligation of the left coronary artery for 30 min was followed by reperfusion. T1 and T2* images were acquired using an 11.7-T magnet before and after intracoronary injection of the contrast agent. A significant increase in signal intensity, visible in those regions containing cardiomyocytes in the early stage of apoptosis, was found. The group of Weissleder also reported on Anx A5-based MRI contrast agents [55], demonstrating the construction of a magneto-optical nanoparticle AnxCLIO-Cy5.5, which was tested in a murine model of transient coronary artery (LAD) occlusion. The synthesis of the probe was achieved in three steps. First, the amino-CLIO nanoparticle was labelled with Cy5.5 and activated with SPDP [*N*-succinimidyl 3-(2-pyridyldithio)propionate], to yield a compound termed 2PySS-CLIO-Cy5.5. Second, Anx A5 was reacted with SATA (*N*-succinimidyl *S*-acetylthioacetate). In the final step of the process, SATAylated Anx A5 was linked with 2PySS-CLIO-Cy5.5 to yield the multimodal AnxCLIO-Cy5.5 nanoparticle. It was demonstrated that it is feasible to obtain high-resolution MR images of cardiomyocyte apoptosis in vivo with the use of the nanoparticle AnxCLIO-Cy5.5.

In early work preformed by our group a fluorescent invasive Anx A5-based imaging protocol for myocardial apoptosis was developed in mice [25]. The promising findings of this study encouraged use of modified human recombinant Anx A5 to construct (Anx A5)-n-1-imono-4-mercaptobutyl, labelled with pertechnetate for clinical studies. One milligram of ^{99m}Tc-Anx A5 (584 MBq) was injected intravenously 2 h after reperfusion in seven AMI patients. In six of the seven patients, increased uptake of ^{99m}Tc-Anx A5 was seen in the infarcted region of the heart

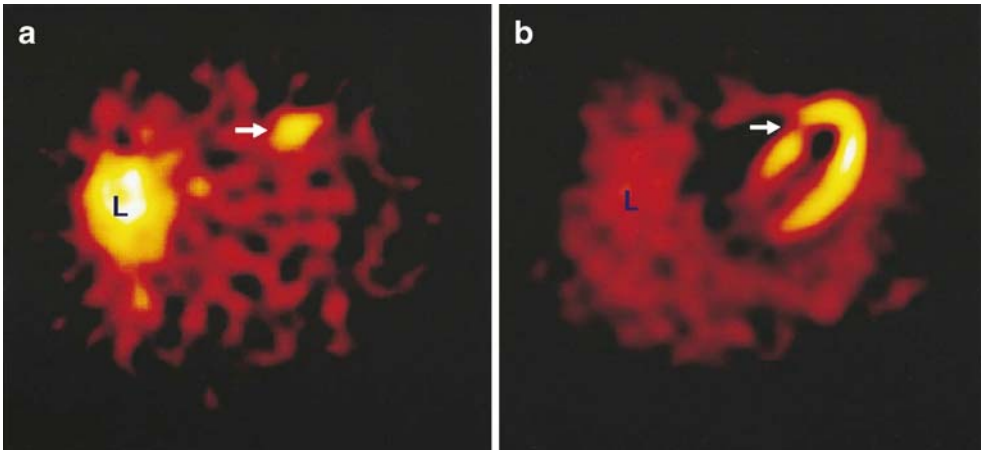

Fig. 2 Transverse tomographic images in a patient with acute anteroseptal infarction. **a** *Arrow* shows increased ^{99m}Tc-labelled Anx A5 uptake in the anteroseptal region 22 h after reperfusion. **b** Perfusion scintigraphy with sestamibi 6–8 weeks after discharge shows an irreversible perfusion defect which coincides with the area of increased ^{99m}Tc-labelled Anx A5 uptake (*arrow*). *L* liver. Reprinted with permission from Elsevier (The Lancet, 2000, 356, 211)

on single-photon emission computed tomography (SPECT) images. No uptake was seen in the heart outside the infarcted area. In all individuals with increased uptake, a matching perfusion defect (on MIBI SPECT) was observed (Figs. 2, 3). These results demonstrated the feasibility of non-invasive monitoring of apoptosis in patients. These techniques may allow measurement not only of the extent of reversible damage but also of the efficacy of novel therapies targeting apoptosis.

Atherosclerotic lesions and plaque instability

Extensive histopathological studies and investigations on the initiation of atherosclerosis in transgenic mice have generated a quite detailed picture of the development of atherosclerosis in the various stages of disease [56–63]. The onset of plaque formation is characterised by circulating levels of oxidised low-density lipoproteins, which are capable of penetrating the endothelial border while inflicting oxidative damage on the endothelial cells in the process. Subsequently, the reactionary expression of inflammatory markers on the endothelial cell surface attracts circulating monocytes to the site of injury, which, upon arrival at the scene, differentiate into macrophages and start ingesting the available lipid and other oxidised particles. Uninhibited intracellular lipid accumulation compromises the function of macrophages and converts them into foam cells [64]. The accompanying secretion of pro-inflammatory cytokines and matrix-metalloproteinases (MMP) likely contributes to the hostility of the plaque environment and weakening of collagen matrix structures, both indirectly through loss of smooth muscle cells and directly through MMP activity [65]. At a certain point, excess damage to macrophages and smooth muscle cells induces apoptosis, causing remnants of lipid-laden dead cells to form small extracellular lipid droplets.

A luxating moment in atherogenesis is thought to occur when the remaining population of functional phagocytes becomes unable to engulf all apoptotic remnants of dying cells in the environment [65]. Once the lesion contains a large, necrotic, lipid pool that is covered by a fibrous cap, primarily consisting of SMCs and extracellular matrix, it is named an atheroma.

A critical finding for vascular risk prediction is that although plaque rupture generally requires progression of lesion size, acute events resulting from rupture may just as

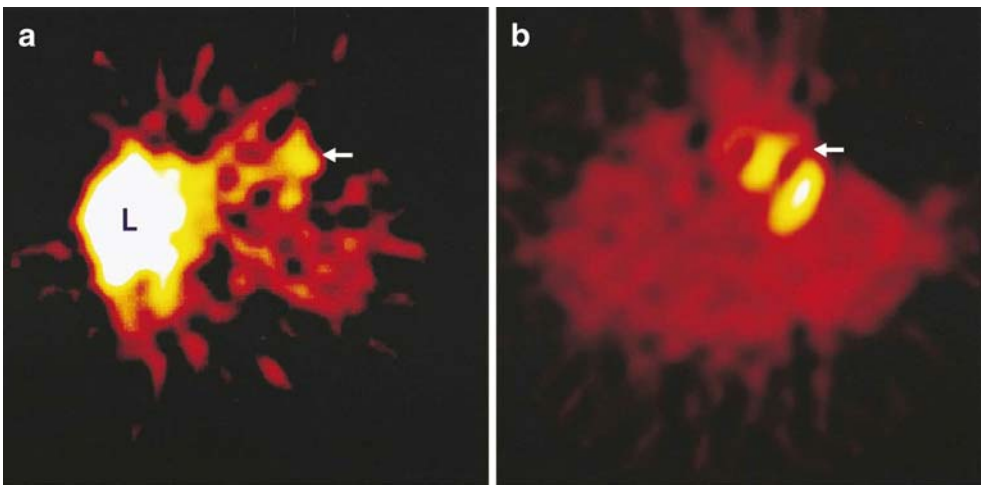

Fig. 3 Transverse tomographic images in a patient with acute anterior wall myocardial infarction. **a** *Arrow* shows increased uptake of ^{99m}Tc-labelled Anx A5 in the infarct area 17.5 h after reperfusion. *L* liver. **b** Perfusion defect on sestamibi perfusion scintigraphy 6–8 weeks after discharge matches the uptake of Anx A5 (*arrow*). Reprinted with permission from Elsevier (The Lancet, 2000, 356, 211)

well originate from only mildly stenotic lesions [66]. Coronary catheterisation studies in patients admitted with acute coronary syndromes have shown that most of the culprit lesions are below the 50% stenosis threshold [67–69]. In reality, the extent of the lesion may be underestimated, since conventional coronary catheterisation does not take the extent of outward remodelling of the coronary artery at the site of atherosclerotic lesions into account. The emerging cardiac multislice CT technology may be better equipped to take outward remodelling into account and to assess the total coronary plaque burden in patients. Nevertheless, these data imply that though plaque dimensions will in general be sufficient for imaging-target visualisation, focussing on mere plaque size entails unsatisfactory prognostic information for clinical use. From a biological perspective, several inflammatory parameters are associated with vulnerable lesions, such as elevated extracellular levels of MMP and pro-inflammatory cytokines, including a variety of interleukins and chemotactic proteins, as has been shown in both experimental and clinical studies [70–73]. Moreover, high-risk lesions are notorious for displaying high levels of inflammation and apoptotic cells; in particular, large amounts of apoptotic macrophages have been found to reside in fragile and ruptured fibrous caps [59, 65, 74]. In 2000, Kolodgie et al. [59] examined 40 culprit lesions from cases of sudden coronary death and reported apoptotic macrophages to constitute up to 50% of the total macrophage population, preferentially localising at the site of rupture. Also, once atheromas have formed, plaques have been found to be far more sensitive to SMC death than regular arterial walls, as recently demonstrated by the group of Bennett [61]. Since all these features share their relation to inflammation and more specifically apoptosis, detection of apoptosis in vivo seems a sensible approach to vulnerable plaque identification. This approach builds on the pivotal role that apoptosis plays in promoting plaque progression and disruption; however, the underlying mechanism is a complex interplay in which apoptosis affects endothelial cells, smooth muscle cells and macrophages in a different manner and with different consequences.

Given the firmly established direct causal relationship between apoptosis and lesion instability [59, 75], in vivo visualisation of the apoptotic plaque status could represent a significant leap forward in the field of therapeutic management for individual patients (Fig. 4).

The expanding knowledge about plaque biology has led to the identification of a variety of potentially suitable molecular markers for vulnerable plaque imaging [76]. Studies have been reported on the targeting of several inflammation-related molecular targets, including vascular adhesion molecules (ICAM1, VCAM1, E-selectin), neoangiogenesis molecules ($\alpha_v\beta_3$ integrin), scavenger receptors on macrophages, MMP proteolytic activity, macrophage metabolic activity and apoptosis (PS) [60, 62, 75–83]. Although some of these approaches have yielded promising experimental data, there is still a paucity of clinical studies confirming the feasibility of these targeted approaches in humans.

Of the clinical results available, the most impressive have been achieved using ^{99m}Tc-Anx A5 SPECT imaging and [^{18}F]fluorodeoxyglucose (^{18}FDG) positron emission tomography (PET) imaging. The latter has been used for many years to detect metabolically hyperactive processes in nuclear oncology. Since the glucose analogue ^{18}FDG is a marker for foci of increased metabolic activity [84] and it is known that macrophages involved in atherosclerotic plaques have a high metabolic rate, there is sound logic behind this strategy. In addition, ^{18}FDG imaging capitalises on the merits of oncological medicine since ^{18}FDG is a

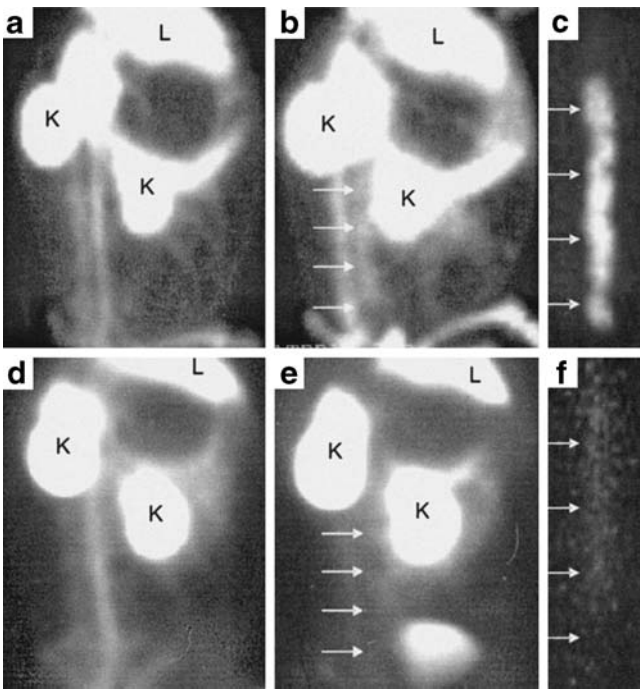

Fig. 4 Feasibility of non-invasive imaging of apoptosis by radiolabelled Anx A5. Left lateral oblique gamma images of experimental atherosclerotic (**a–c**) and control (**d–f**) rabbits injected with ^{99m}Tc-Anx A5; *L* and *K* indicate liver and kidney activities, respectively. Images at the time of injection (**a, d**) and at 2 h after injection (**b, e**) are shown. Although blood pool activity is seen at the time of injection (**a**) in the atherosclerotic animal, tracer uptake is clearly visible in the abdominal aorta (with lesions) at 2 h (**b**). **c** Ex vivo image of **b** shows intense ^{99m}Tc-Anx A5 uptake in the arch and abdominal region. Annexin-positive areas were confirmed to contain macrophage- and apoptosis-rich regions in the atherosclerotic plaque by histology. **d–f** show the corresponding images in the control animal. Note that the aorta is indistinguishable from background at 2 h after injection (**e**). The blood pool at the time of injection in the control animal (**d**) is comparable to that in the atherosclerotic animal. **f** Ex vivo aortic image of the control animal demonstrates the absence of ^{99m}Tc-labelled Anx A5 uptake. From Kolodgie et al. [75]

clinically approved tracer that can be detected with high sensitivity and accuracy by PET technology, whereas PET conjugates for most alternative plaque imaging targets are still in the process of development. ^{18}FDG imaging of arterial inflammation has been performed with rather promising results in retrospective studies of oncological ^{18}FDG scans, in experimental settings and in in vivo clinical studies by Rudd and colleagues [76, 82, 85, 86]. In an eight-patient pilot study, they were able to correlate ^{18}FDG uptake in carotid lesions of patients scheduled for endarterectomy with histologically assessed macrophage density ($p<0.005$). However, a practical difficulty of performing ^{18}FDG imaging in the search for coronary lesion instability lies in the physical activity of the cardiac muscle, which results in high glucose requirements and thus severe background signal.

In addition to detection of the vulnerable plaque with ^{18}FDG, imaging of the vulnerable plaque with ^{99m}Tc-Anx A5 has yielded some exciting results as well. The first demonstration of the feasibility of in vivo imaging of plaque instability with ^{99m}Tc-Anx A5, in animals, was given in 2003 by Kolodgie et al. It was demonstrated in a rabbit model of aortic de-endothelialisation followed by a high-fat diet that ^{99m}Tc-Anx A5 showed a ninefold higher binding to the atherosclerotic vessels than to the control vessels [75]. Further validation of the Anx A5 imaging concept in the vulnerable plaque was done by Johnson and colleagues in 2005 [87]. In a porcine model of atherosclerosis the feasibility of SPECT imaging with ^{99m}Tc-Anx A5 to assess atheroma progression in coronary arteries was demonstrated. This was ultimately challenging owing to the low mass of the imaging target and cardiopulmonary motion. As swine and human hearts have similar cardiac dimensions, these results indicate that non-invasive functional imaging of coronary plaque instability could be realistic in the near future. The first clinical demonstration of the feasibility of nuclear vulnerable plaque imaging with ^{99m}Tc-Anx A5 was given by Kietselaer et al. in 2004 [43]. In a pilot study, four patients were included who were scheduled for carotid endarterectomy and had a history of recent ($n=2$) or remote ($n=2$) transient ischaemic attack (TIA). Before surgery ^{99m}Tc-Anx A5 was administered and SPECT imaging was performed. In the two patients who had suffered a TIA more than 3 months before imaging and had since been treated with statins and antiplatelet agents, no tracer uptake of Anx A5 was observed (Fig. 5). Histological analysis confirmed stable lesions with negligible macrophage infiltration and intra-plaque haemorrhage. In contrast, the two patients who had experienced transient ischaemia shortly before imaging (3 and 4 days, respectively) demonstrated marked uptake of Anx A5 in the culprit carotid vessel, while the contralateral arteries remained clear of tracer binding. Anx A5 binding was histologically localised to apoptotic macrophage membranes. An interesting finding during this study was that echo-Doppler examination in one of the patients with a recent TIA identified a severe stenotic lesion in the contralateral carotid artery prior to imaging. On the ^{99m}Tc-Anx A5 scan, however, the lesion was negative, though it might have been suspected as the culprit lesion by conventional techniques. This finding underlines the potential added value of functional versus anatomical imaging in predicting the likelihood of future thrombotic events.

Among the discussed imaging modalities for vulnerable plaque detection, nuclear imaging (PET in particular) is far superior to MRI, being capable of detecting probes at the picomolar range [88]. PET further outperforms SPECT imaging regarding spatial resolution, with 4- to 6-mm versus 10- to 15-mm resolution in the centre of the field. The major difficulty in evaluating PET or SPECT usually originates from orientation and localisation of the measured signal in the body. To overcome this, nuclear imaging modalities can be co-registered and overlaid with conventional CT or MRI imaging, hence providing anatomical landmarks in relation to molecular information. Improve-

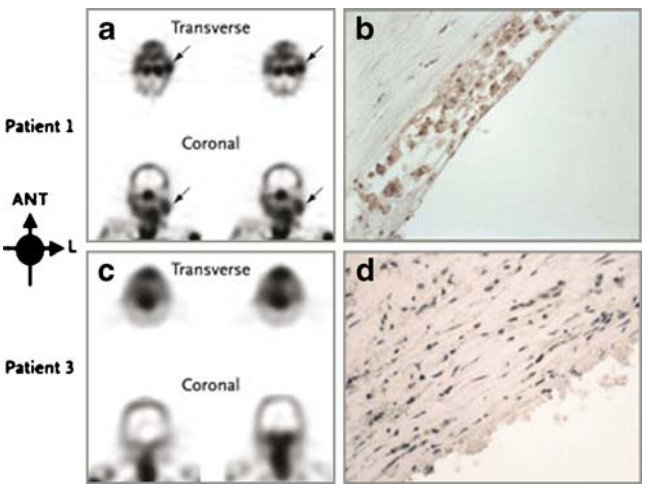

Fig. 5 Images of unstable atherosclerotic carotid artery lesions obtained with radiolabelled Anx A5. **a** Transverse and coronal views obtained by SPECT in patient 1, who had a left-sided TIA 3 days before imaging. Although this patient had clinically significant stenosis of both carotid arteries, uptake of radiolabelled Anx A5 is evident only in the culprit lesion (*arrows*). **b** Histopathological analysis of an endarterectomy specimen from patient 1 (polyclonal rabbit anti-Anx A5 antibody, ×400) shows substantial infiltration of macrophages into the neointima, with extensive binding of Anx A5 (brown). **c** In contrast, SPECT images of patient 3, who had had a right-sided TIA 3 months before imaging, do not show evidence of Anx A5 uptake in the carotid artery region on either side. Doppler ultrasonography revealed a clinically significant obstructive lesion on the affected side. **d** Histopathological analysis of an endarterectomy specimen from patient 3 (polyclonal rabbit anti-Anx A5 antibody, ×400) shows a lesion rich in smooth muscle cells, with negligible binding of Anx A5. *ANT* anterior, *L* left. [43]

ments in the availability and costs of PET/CT or PET/MRI imaging devices will therefore imply great advantages. Given the high costs of imaging, diagnostic algorithms in the future most likely will combine relatively cheap serum biomarkers that indicate plaque instability with the subsequent use of expensive imaging technology in selected cases. This indicates that the specific niche for both serum and imaging biomarkers needs to be defined in large prospective studies. In addition, much is to be gained from refinements of the radioligand with regard to blood clearance and biodistribution, since molecular imaging typically requires fast binding of the probe to the target, rapid subsequent clearance from the blood and not too short radioactive half-lives.

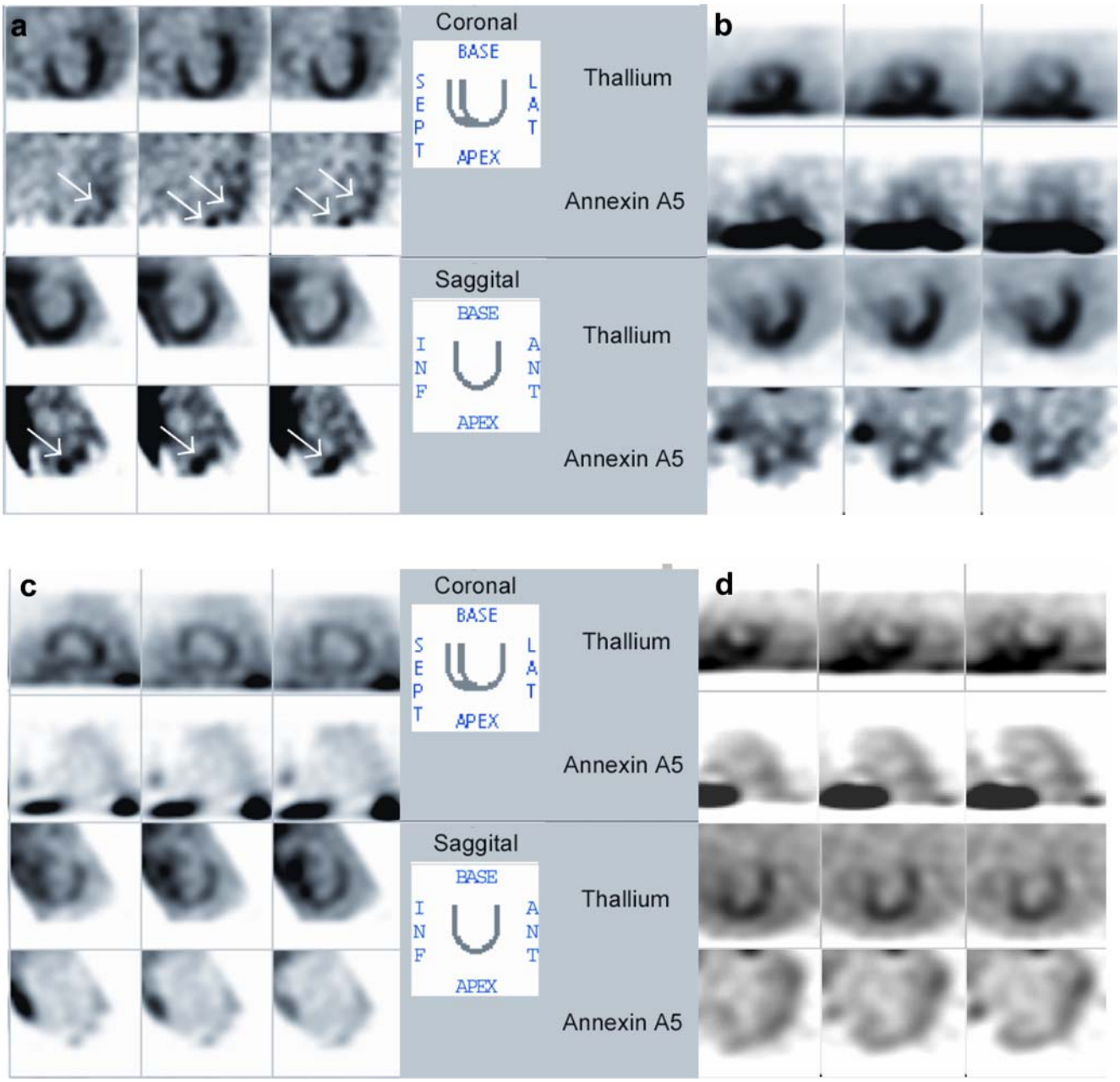

Fig. 6 Dual-isotope imaging using 201Tl for left ventricular contour detection and, simultaneously, radiolabeled annexin A5 in patients with dilated cardiomyopathy. **a** Dilated cardiomyopathy patient with rapid deterioration of left ventricular function. Note focal uptake in apex and lateral wall, and slight septal uptake. **b** Dilated cardiomyopathy patient in acute heart failure. Note global uptake of radiolabeled annexin A5. **c** Dilated cardiomyopathy patient in stable clinical condition. Uptake is absent even when image is enhanced to the extent that background radioactivity can be observed. **d** Family member of patient in panel **b**. No clinical evidence is seen of dilated cardiomyopathy. Note absence of uptake of radiolabeled annexin A5. *ANT*, anterior; *INF*, inferior; *LAT*, lateral; *SEPT*, septal. Reprinted by permission of the Society of Nuclear Medicine from [90]

Heart failure

Heart failure (HF) is growing to epidemic proportions, partially due to the better treatment of AMI. The pathogenesis of heart failure is still poorly understood. There may be an important role for cell death in the progression of congestive HF. A number of papers have reported on the differences in the amount of cell death in healthy and failing hearts. The baseline rate of apoptosis in healthy human hearts is around one to ten cardiac myocytes per 10^5 nuclei. On the other hand, 80–250 heart muscle cells per 10^5 cardiac nuclei undergo apoptosis at any given time in late-stage dilated cardiomyopathy. However, it remains unclear whether this cell death is a coincidental finding, a protective process or a causal component in the pathogenesis. In work done by Wencker and co-workers, the uncertainty of the role of cell death was addressed. In a transgenic mouse model with a conditionally active caspase expressed exclusively in the myocardium, they demonstrated that even very low levels of cardiomyocyte apoptosis

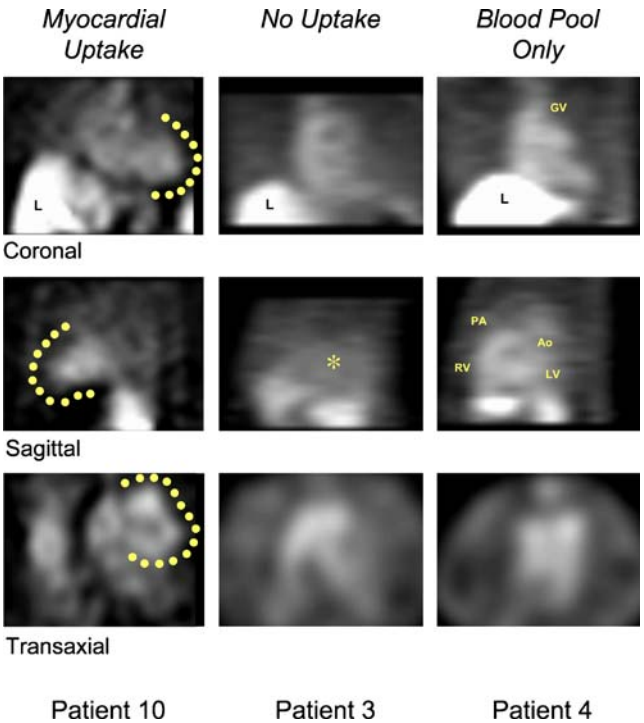

Fig. 7 SPECT images of ^{99m}Tc-labelled Anx A5 in three patients (10, 3 and 4) are demonstrated. **a** In patient 10, myocardial uptake (as outlined by *solid circles*) is clearly seen in all tomographic orientations and can be differentiated from the left ventricular cavity, especially in the transaxial slice. **b** In patient 3, by contrast, no Anx A5 uptake is observed, and only background activity is seen. **c** Patient 4 demonstrates Anx A5 activity in the blood pool originating from the great vessels (*GV* great cardiac vein, *PA* pulmonary artery, *Ao* aorta) and ventricular contours, but no activity is observed in the myocardium. The scan of patient 10, with myocardial uptake, was further processed (Fig. 8). *RV* right ventricle, *LV* left ventricle. Adapted by permission from Macmillan Publishers Ltd: Nature Medicine [42], copyright 2001

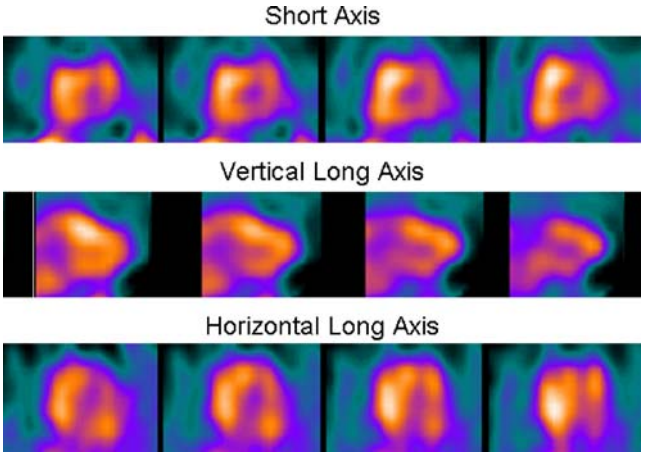

Fig. 8 Diffuse myocardial uptake of ^{99m}Tc-labelled Anx A5 in cardiac allograft. Patient 10 underwent Anx A5 imaging 9 months after orthotopic heart transplantation. SPECT imaging 3 h after intravenous injection of radiolabelled Anx A5 demonstrated multifocal myocardial uptake of radiotracer. Smoothing of the images and cardiac SPECT processing in the short axis, vertical long axis and horizontal long axis revealed myocardial perfusion scan-like images with diffuse uptake in the whole myocardium, suggesting apoptosis in the myocardium. Adapted by permission from Macmillan Publishers Ltd: Nature Medicine [42], copyright 2001

(23 per 10^5 nuclei, compared with 1.5 per 10^5 nuclei in controls) caused a lethal dilated cardiomyopathy. Inhibition of this active caspase largely prevented the development of cardiac dilation and contractile dysfunction. These and other data suggest that cardiomyocyte apoptosis and necrosis may be a causal mechanism of heart failure, contributing to adverse left ventricle (LV) remodelling. Inhibition of this cell death process may constitute the basis for novel therapies. Consequently, anti-apoptotic agents have been developed and tested in animal models of HF with promising results [89].

Although, as discussed earlier, it is possible to detect cell death in MI leading to HF, the small amount of cell death present in heart failure (80–250 cardiomyocytes per 10^5 cardiac nuclei) makes detection with the current techniques very challenging. However, the feasibility of detecting apoptosis in patients with progressive idiopathic dilated cardiomyopathy was demonstrated in a proof of principle study done by Kietselaer [90]. Nine patients with idiopathic dilated cardiomyopathy (IDCM) were evaluated, as well as two family members with hypertrophic cardiomyopathy in different stages of disease. Patients were imaged with ^{99m}Tc-labelled Anx A5. ^{201}Tl images were used for orientation. Other causes of IDCM were excluded using laboratory testing, echocardiography and coronary angiography. It was found that five patients with IDCM showed focal uptake of radiolabelled Anx A5 and that one patient showed global uptake in the left ventricle (Fig. 6, left panel). No enhanced uptake could be visualised in the other six patients (Fig. 6) and controls. All cases that showed

Anx A5 uptake in the heart displayed recent onset or recent worsening of left ventricular function and functional class. In cases that did not show Anx A5 uptake, LV function and clinical status remained stable. Kietselaer concluded that non-invasive imaging using ^{99m}Tc-Anx A5 detects apoptosis in patients suffering from IDCM, providing further evidence for the role of apoptosis in the pathogenesis of IDCM. In addition, Anx A5 imaging identifies high-risk patients who might benefit from cell death blocking strategies.

In addition to imaging of apoptosis, the detection of the molecular substrates of early-stage alterations leading to HF, such as vascular remodelling in infarcted tissue, is an emerging technique. Vascular remodelling is associated with non-contractile scar tissue formation that may contribute to adverse LV remodelling. However, none of these molecular techniques has reached the clinical stage yet.

Cardiac allograft rejection

Until 1997, almost 46,300 heart transplantations had been carried out worldwide [48]. Despite this encouraging number, only 50% of cardiac transplant recipients will survive 10 years and almost all will die within 20 years unless re-transplantation is preformed [19]. One of the possible complications for patients who have received a donor heart is transplant rejection. Under the current medical guidelines, endomyocardial biopsies (EMBs) are recommended 15–20 times in the first year after transplantation to monitor potential allograft rejection. EMB is an invasive diagnostic procedure and not without risk of complications. Allograft rejection is pathologically characterised by perivascular and interstitial mononuclear inflammatory cell infiltration associated with myocyte necrosis and apoptosis [91, 92]. Because the process of apoptosis can be pharmaceutically manipulated, identifying apoptosis non-invasively is of critical importance [93].

In a study done by Narula and co-workers [42], 18 patients who had undergone heart transplantation within the past year were subjected to non-invasive imaging with Anx A5. Patients received an injected dose of 555–1,110 MBq (15–30 mCi) of ^{99m}Tc-Anx A5 and underwent SPECT imaging 1 h after injection (Fig. 7). In 13 out of these 18 patients, no myocardial uptake of ^{99m}Tc-Anx A5 was observed. In the remaining five patients, uptake of ^{99m}Tc-Anx A5 in the myocardial region was observed, which was associated with at least moderate transplant rejection (Fig. 8), of International Society of Heart and Lung Transplantation (ISHLT) grade 2/4. Histological analysis revealed active caspase-3 in EMB specimens. This study demonstrated the clinical feasibility of detecting cardiac allograft rejection induced apoptosis, which, after confirming these findings in larger clinical studies, might lead to a reduction for the need of EMBs.

Future perspectives

Of all the apoptotic imaging agents, Anx A5 has made the most successful transition from the test tube to the clinical arena. Novel imaging modalities like PET/CT and SPECT/CT are making a significant contribution to the growing role of molecular imaging. The combination of anatomical imaging with CT and biological imaging using SPECT or PET yields a new synergistic imaging modality that provides detailed information on the molecular (patho) physiological processes in relation to exact anatomical orientation.

The next challenge is to assess the incremental clinical value of molecular imaging and its ability to change patient management decisions. For this purpose, prospective cohort studies need to be designed to evaluate the clinical meaning of molecular imaging scan results in relation to the progression of the underlying disease. For instance, data on the association between Anx A5 uptake in plaques in the carotid arteries and clinical event rate are still lacking. The availability of such large clinical datasets may allow for better stratification of patients and therefore more optimal treatment decisions.

Finally, we and others have found that not only apoptotic cells but also viable cells are detectable with Anx A5. Our work on the vulnerable plaque showed that several processes leading to plaque instability are associated with PS expression, such as activated macrophages (inflammation) and aging red blood cells (intra-plaque haemorrhage). This ability of Anx A5 to visualise exposed PS in different biological conditions opens novel opportunities for imaging.

References

1. Narula J, Baliga R. What's in a name? Would that which we call death by any other name be less tragic? Ann Thorac Surg 2001;72(5):1454–6.
2. Cotran RS, Kumar V, Collins T, Robbins SL. Robbins pathologic basis of disease, 6th ed. Philadelphia: W.B. Saunders, 1999. p 1424, xv.
3. Kerr JF, Wyllie AH, Currie AR. Apoptosis: a basic biological phenomenon with wide-ranging implications in tissue kinetics. Br J Cancer 1972;26(4):239–57.
4. Leist M, Jaättelä M. Four deaths and a funeral: from caspases to alternative mechanisms. Nat Rev Mol Cell Biol 2001;2(8):589–98.
5. Gudkov AV, Komarova EA. The role of p53 in determining sensitivity to radiotherapy. Nat Rev Cancer 2003;3(2):117–29.
6. Okada H, Mak TW. Pathways of apoptotic and non-apoptotic death in tumour cells. Nat Rev Cancer 2004;4(8):592–603.

7. Brown JM, Attardi LD. The role of apoptosis in cancer development and treatment response. Nat Rev Cancer 2005;5(3): 231–7.
8. Castedo M, Perfettini JL, Roumier T, et al. Cell death by mitotic catastrophe: a molecular definition. Oncogene 2004;23(16): 2825–37.
9. Klionsky DJ, Emr SD. Autophagy as a regulated pathway of cellular degradation. Science 2000;290 5497:1717–21.
10. Gozuacik D, Kimchi A. Autophagy as a cell death and tumor suppressor mechanism. Oncogene 2004;23(16):2891–906.
11. Edinger AL, Thompson CB. Defective autophagy leads to cancer. Cancer Cell 2003;4(6):422–4.
12. Kunapuli S, Rosanio S, Schwarz ER. How do cardiomyocytes die? Apoptosis and autophagic cell death in cardiac myocytes. J Card Fail 2006;12 5:381–91.
13. Van Cruchten S, Van Den Broeck W. Morphological and biochemical aspects of apoptosis, oncosis and necrosis. Anat Histol Embryol 2002;31(4):214–23.
14. Kroemer G, El-Deiry WS, Golstein P, et al. Classification of cell death: recommendations of the Nomenclature Committee on cell death. Cell Death Differ 2005;12 Suppl 2:1463–7.
15. Scarabelli TM, Knight R, Stephanou A, et al. Clinical implications of apoptosis in ischemic myocardium. Curr Probl Cardiol 2006;31 (3):181–264.
16. Shi Y. Caspase activation, inhibition, and reactivation: a mechanistic view. Protein Sci 2004;13(8):1979–87.
17. Stefflova K, Chen J, Li H, et al. Targeted photodynamic therapy agent with a built-in apoptosis sensor for in vivo near-infrared imaging of tumor apoptosis triggered by its photosensitization in situ. Mol Imaging 2006;5(4):520–32.
18. Bhojani MS, Hamstra DA, Chang DC, et al. Imaging of proteolytic activity using a conditional cell surface receptor. Mol Imaging 2006;5(2):129–37.
19. Darzynkiewicz Z, Bedner E, Smolewski P, et al. Detection of caspases activation in situ by fluorochrome-labeled inhibitors of caspases (FLICA). Methods Mol Biol 2002;203:289–99.
20. Fadok VA, Bratton DL, Rose DM, et al. A receptor for phosphatidylserine-specific clearance of apoptotic cells. Nature 2000;405(6782):85–90.
21. Zwaal RF, Schroit AJ. Pathophysiologic implications of membrane phospholipid asymmetry in blood cells. Blood 1997;89 (4):1121–32.
22. Martin SJ, Reutelingsperger CP, McGahon AJ, et al. Early redistribution of plasma membrane phosphatidylserine is a general feature of apoptosis regardless of the initiating stimulus: inhibition by overexpression of Bcl-2 and Abl. J Exp Med 1995;182(5):1545–56.
23. Blankenberg FG, Katsikis PD, Tait JF, et al. In vivo detection and imaging of phosphatidylserine expression during programmed cell death. Proc Natl Acad Sci U S A 1998;95(11):6349–54.
24. Dumont EA, Hofstra L, van Heerde WL, et al. Cardiomyocyte death induced by myocardial ischemia and reperfusion: measurement with recombinant human annexin-V in a mouse model. Circulation 2000;102(13):1564–8.
25. Dumont EA, Reutelingsperger CP, Smits JF, et al. Real-time imaging of apoptotic cell-membrane changes at the single-cell level in the beating murine heart. Nat Med 2001;7(12):1352–5.
26. Hofstra L, Liem IH, Dumont EA, et al. Visualisation of cell death in vivo in patients with acute myocardial infarction. Lancet 2000; 356(9225):209–12.
27. Verhoven B, Schlegel RA, Williamson P. Mechanisms of phosphatidylserine exposure, a phagocyte recognition signal, on apoptotic T lymphocytes. J Exp Med 1995;182(5):1597–601.
28. Tait JF, Gibson D. Measurement of membrane phospholipid asymmetry in normal and sickle-cell erythrocytes by means of annexin V binding. J Lab Clin Med 1994;123(5):741–8.
29. Koopman G, Reutelingsperger CP, Kuijten GA, et al. Annexin V for flow cytometric detection of phosphatidylserine expression on B cells undergoing apoptosis. Blood 1994;84(5):1415–20.
30. Gerke V, Moss SE. Annexins: from structure to function. Physiol Rev 2002;82(2):331–71.
31. Moss SE, Morgan RO. The annexins. Genome Biol 2004;5 (4):219.
32. Hayes MJ, Moss SE. Annexins and disease. Biochem Biophys Res Commun 2004;322(4):1166–70.
33. Reutelingsperger CP. Annexins: key regulators of haemostasis, thrombosis, and apoptosis. Thromb Haemost 2001;86(1):413–9.
34. Hayes MJ, Rescher U, Gerke V, et al. Annexin-actin interactions. Traffic 2004;5(8):571–6.
35. Fadok VA, Voelker DR, Campbell PA, et al. Exposure of phosphatidylserine on the surface of apoptotic lymphocytes triggers specific recognition and removal by macrophages. J Immunol 1992;148(7):2207–16.
36. van Engeland M, Kuijpers HJ, Ramaekers FC, et al. Plasma membrane alterations and cytoskeletal changes in apoptosis. Exp Cell Res 1997;235(2):421–30.
37. Kenis H, van Genderen H, Bennaghmouch A, et al. Cell surface-expressed phosphatidylserine and annexin A5 open a novel portal of cell entry. J Biol Chem 2004;279(50):52623–9.
38. Vriens PW, Blankenberg FG, Stoot JH, et al. The use of technetium Tc 99m annexin V for in vivo imaging of apoptosis during cardiac allograft rejection. J Thorac Cardiovasc Surg 1998;116(5):844–53.
39. Post AM, Katsikis PD, Tait JF, et al. Imaging cell death with radiolabeled annexin V in an experimental model of rheumatoid arthritis. J Nucl Med 2002;43(10):1359–65.
40. Glaser M, Collingridge DR, Aboagye EO, et al. Iodine-124 labelled annexin-V as a potential radiotracer to study apoptosis using positron emission tomography. Appl Radiat Isot 2003;58 (1):55–62.
41. Murakami Y, Takamatsu H, Taki J, et al. ^{18}F-labelled annexin V: a PET tracer for apoptosis imaging. Eur J Nucl Med Mol Imaging 2004;31(4):469–74.
42. Narula J, Acio ER, Narula N, et al. Annexin-V imaging for noninvasive detection of cardiac allograft rejection. Nat Med 2001;7(12):1347–52.
43. Kietselaer BL, Reutelingsperger CP, Heidendal GA, et al. Noninvasive detection of plaque instability with use of radiolabeled annexin A5 in patients with carotid-artery atherosclerosis. N Engl J Med 2004;350(14):1472–3.
44. Hofstra L, Dumont EA, Thimister PW, et al. In vivo detection of apoptosis in an intracardiac tumor. JAMA 2001;285(14):1841–2.
45. van de Wiele C, Lahorte C, Vermeersch H, et al. Quantitative tumor apoptosis imaging using technetium-99m-HYNIC annexin V single photon emission computed tomography. J Clin Oncol 2003;21(18):3483–7.
46. Boersma HH, Liem IH, Kemerink GJ, et al. Comparison between human pharmacokinetics and imaging properties of two conjugation methods for ^{99m}Tc-annexin A5. Br J Radiol 2003;76 (908):553–60.
47. Zhao M, Beauregard DA, Loizou L, et al. Non-invasive detection of apoptosis using magnetic resonance imaging and a targeted contrast agent. Nat Med 2001;7(11):1241–4.
48. Zhao M, Zhu X, Ji S, et al. ^{99m}Tc-labeled C2A domain of synaptotagmin I as a target-specific molecular probe for noninvasive imaging of acute myocardial infarction. J Nucl Med 2006;47 (8):1367–74.
49. Haberkorn U, Kinscherf R, Krammer PH, et al. Investigation of a potential scintigraphic marker of apoptosis: radioiodinated Z-Val-Ala-DL-Asp(*O*-methyl)-fluoromethyl ketone. Nucl Med Biol 2001;28(7):793–8.

50. Kopka K, Faust A, Keul P, et al. 5-Pyrrolidinylsulfonyl isatins as a potential tool for the molecular imaging of caspases in apoptosis. J Med Chem 2006;49(23):6704–15.
51. Damianovich M, Ziv I, Heyman SN, et al. ApoSense: a novel technology for functional molecular imaging of cell death in models of acute renal tubular necrosis. Eur J Nucl Med Mol Imaging 2006;33(3):281–91.
52. Aloya R, Shirvan A, Grimberg H, et al. Molecular imaging of cell death in vivo by a novel small molecule probe. Apoptosis 2006;11 (12):2089–101.
53. Freude B, Masters TN, Kostin S, et al. Cardiomyocyte apoptosis in acute and chronic conditions. Basic Res Cardiol 1998;93 (2):85–9.
54. Hiller KH, Waller C, Nahrendorf M, et al. Assessment of cardiovascular apoptosis in the isolated rat heart by magnetic resonance molecular imaging. Mol Imaging 2006;5(2):115–21.
55. Sosnovik DE, Schellenberger EA, Nahrendorf M, et al. Magnetic resonance imaging of cardiomyocyte apoptosis with a novel magneto-optical nanoparticle. Magn Reson Med 2005;54(3): 718–24.
56. Libby P. Inflammation in atherosclerosis. Nature 2002;420 (6917):868–74.
57. Virmani R, Moll FL, Koekkoek JA, et al. Atherosclerotic plaque progression and vulnerability to rupture: angiogenesis as a source of intraplaque hemorrhage. Arterioscler Thromb Vasc Biol 2005;25(10):2054–61.
58. Kolodgie FD, Burke AP, Farb A, et al. The thin-cap fibroatheroma: a type of vulnerable plaque: the major precursor lesion to acute coronary syndromes. Curr Opin Cardiol 2001;16(5):285–92.
59. Kolodgie FD, Narula J, Burke AP, et al. Localization of apoptotic macrophages at the site of plaque rupture in sudden coronary death. Am J Pathol 2000;157(4):1259–68.
60. Narula J, Strauss HW. Imaging of unstable atherosclerotic lesions. Eur J Nucl Med Mol Imaging 2005;32(1):1–5.
61. Clarke MC, Figg N, Maguire JJ, et al. Apoptosis of vascular smooth muscle cells induces features of plaque vulnerability in atherosclerosis. Nat Med 2006;12(9):1075–80.
62. Tsimikas S, Shortal BP, Witztum JL, et al. In vivo uptake of radiolabeled MDA2, an oxidation-specific monoclonal antibody, provides an accurate measure of atherosclerotic lesions rich in oxidized LDL and is highly sensitive to their regression. Arterioscler Thromb Vasc Biol 2000;20(3):689–97.
63. Virmani R, Burke AP, Farb A, et al. Pathology of the vulnerable plaque. J Am Coll Cardiol 2006;47(8 Suppl):C13–8.
64. Steinberg D, Lewis A. Conner Memorial Lecture. Oxidative modification of LDL and atherogenesis. Circulation 1997;95 (4):1062–71.
65. Tabas I. Consequences and therapeutic implications of macrophage apoptosis in atherosclerosis. The importance of lesion stage and phagocytic efficiency. Arterioscler Thromb Vasc Biol 2005;25 (11):2255–64.
66. Falk E, Shah PK, Fuster V. Coronary plaque disruption. Circulation 1995;92(3):657–71.
67. Giroud D, Li JM, Urban P, et al. Relation of the site of acute myocardial infarction to the most severe coronary arterial stenosis at prior angiography. Am J Cardiol 1992;69(8):729–32.
68. Little WC. Angiographic assessment of the culprit coronary artery lesion before acute myocardial infarction. Am J Cardiol 1990;66 (16):44G–47G.
69. Little WC, Applegate RJ. Role of plaque size and degree of stenosis in acute myocardial infarction. Cardiol Clin 1996;14 (2):221–8.
70. Kai H, Ikeda H, Yasukawa H, et al. Peripheral blood levels of matrix metalloproteases-2 and -9 are elevated in patients with acute coronary syndromes. J Am Coll Cardiol 1998;32(2):368–72.
71. Ikeda U, Matsui K, Murakami Y, et al. Monocyte chemoattractant protein-1 and coronary artery disease. Clin Cardiol 2002;25 (4):143–7.
72. Ridker PM, Rifai N, Rose L, et al. Comparison of C-reactive protein and low-density lipoprotein cholesterol levels in the prediction of first cardiovascular events. N Engl J Med 2002; 347(20):1557–65.
73. Cybulsky MI, Gimbrone MA Jr. Endothelial expression of a mononuclear leukocyte adhesion molecule during atherogenesis. Science 1991;251(4995):788–91.
74. Kockx MM, Herman AG. Apoptosis in atherosclerosis: beneficial or detrimental? Cardiovasc Res 2000;45(3):736–46.
75. Kolodgie FD, Petrov A, Virmani R, et al. Targeting of apoptotic macrophages and experimental atheroma with radiolabeled annexin V: a technique with potential for noninvasive imaging of vulnerable plaque. Circulation 2003;108(25):3134–9.
76. Choudhury RP, Fuster V, Fayad ZA. Molecular, cellular and functional imaging of atherothrombosis. Nat Rev Drug Discov 2004;3(11):913–25.
77. Sadeghi MM, Schechner JS, Krassilnikova S, et al. Vascular cell adhesion molecule-1-targeted detection of endothelial activation in human microvasculature. Transplant Proc 2004;36(5):1585–91.
78. Sibson NR, Blamire AM, Bernades-Silva M, et al. MRI detection of early endothelial activation in brain inflammation. Magn Reson Med 2004;51(2):248–52.
79. Ohtsuki K, Hayase M, Akashi K, et al. Detection of monocyte chemoattractant protein-1 receptor expression in experimental atherosclerotic lesions: an autoradiographic study. Circulation 2001;104(2):203–8.
80. Iuliano L, Mauriello A, Sbarigia E, et al. Radiolabeled native low-density lipoprotein injected into patients with carotid stenosis accumulates in macrophages of atherosclerotic plaque: effect of vitamin E supplementation. Circulation 2000;101(11):1249–54.
81. Schafers M, Riemann B, Kopka K, et al. Scintigraphic imaging of matrix metalloproteinase activity in the arterial wall in vivo. Circulation 2004;109(21):2554–9.
82. Rudd JH, Warburton EA, Fryer TD, et al. Imaging atherosclerotic plaque inflammation with [^{18}F]-fluorodeoxyglucose positron emission tomography. Circulation 2002;105(23):2708–11.
83. Winter PM, Morawski AM, Caruthers SD, et al. Molecular imaging of angiogenesis in early-stage atherosclerosis with alpha (v)beta3-integrin-targeted nanoparticles. Circulation 2003;108 (18):2270–4.
84. Yamada S, Kubota K, Kubota R, et al. High accumulation of fluorine-18-fluorodeoxyglucose in turpentine-induced inflammatory tissue. J Nucl Med 1995;36(7):1301–6.
85. Lederman RJ, Raylman RR, Fisher SJ, et al. Detection of atherosclerosis using a novel positron-sensitive probe and 18-fluorodeoxyglucose (FDG). Nucl Med Commun 2001;22(7):747–53.
86. Vallabhajosula S, Machac K, Knesaurek J. Imaging atherosclerotic macrophage density by positron emission tomography using F-18 flurodeoxyglucose (FDG) [abstract]. J Nucl Med 1996;38P.
87. Johnson LL, Schofield L, Donahay T, et al. ^{99m}Tc-annexin V imaging for in vivo detection of atherosclerotic lesions in porcine coronary arteries. J Nucl Med 2005;46(7):1186–93.
88. Strauss HW, Grewal RK, Pandit-Taskar N. Molecular imaging in nuclear cardiology. Semin Nucl Med 2004;34(1):47–55.
89. Wencker D, Chandra M, Nguyen K, et al. A mechanistic role for cardiac myocyte apoptosis in heart failure. J Clin Invest 2003;111 (10):1497–504.
90. Kietselaer BL, Reutelingsperger CP, Boersma HH, et al. Noninvasive detection of programmed cell loss with 99mTc-

labeled annexin A5 in heart failure. J Nucl Med 2007; 48 (4):562–7.
91. Laguens RP, Meckert PM, Martino JS, et al. Identification of programmed cell death (apoptosis) in situ by means of specific labeling of nuclear DNA fragments in heart biopsy samples during acute rejection episodes. J Heart Lung Transplant 1996;15 (9):911–8.
92. Szabolcs MJ, Ravalli S, Minanov O, et al. Apoptosis and increased expression of inducible nitric oxide synthase in human allograft rejection. Transplantation 1998;65(6):804–12.
93. Puig M, Ballester M, Matias-Guiu X, et al. Burden of myocardial damage in cardiac allograft rejection: scintigraphic evidence of myocardial injury and histologic evidence of myocyte necrosis and apoptosis. J Nucl Cardiol 2000;7(2):132–9.